Chitosan-based dressings loaded with neurotensin—an efficient strategy to improve early diabetic wound healing

Liane I.F. Moura [a,b], Ana M.A. Dias [b], Ermelindo C. Leal [a], Lina Carvalho [c], Hermínio C. de Sousa [b,*], Eugénia Carvalho [a,d,*]

[a] Center of Neuroscience and Cell Biology, University of Coimbra, 3004-517 Coimbra, Portugal
[b] CIEPQPF, Chemical Engineering Department, FCTUC, University of Coimbra, Rua Sílvio Lima, Pólo II – Pinhal de Marrocos, 3030-790 Coimbra, Portugal
[c] Institute of Pathology, Faculty of Medicine, University of Coimbra, 3004-517 Coimbra, Portugal
[d] APDP, The Portuguese Diabetes Association, Rua do Salitre, no. 118-120, 1250-203 Lisboa, Portugal

ARTICLE INFO

ABSTRACT

One important complication of diabetes mellitus is chronic, non-healing diabetic foot ulcers (DFUs). This study aims to develop and use dressings based on chitosan derivatives for the sustained delivery of neurotensin (NT), a neuropeptide that acts as an inflammatory modulator in wound healing. Three different derivatives, namely N-carboxymethyl chitosan, 5-methyl pyrrolidinone chitosan (MPC) and N-succinyl chitosan, are presented as potential biomaterials for wound healing applications. Our results show that MPC has the best fluid handling capacity and delivery profile, also being non-toxic to Raw 264.7 and HaCaT cells. NT-loaded and non-loaded MPC dressings were applied to control/diabetic wounds to evaluate their in vitro/in vivo performance. The results show that the former induced more rapid healing (50% wound area reduction) in the early phases of wound healing in diabetic mice. A NT-loaded MPC foam also reduced expression of the inflammatory cytokine TNF-α ($P < 0.001$) and decreased the amount of inflammatory infiltrate on day 3. On day 10 MMP-9 was reduced in diabetic skin ($P < 0.001$), significantly increasing fibroblast migration and collagen (COL1A1, COL1A2 and COL3A1) expression and deposition. These results suggest that MPC-based dressings may work as an effective support for sustained NT release to reduce DFUs.

© 2013 Acta Materialia Inc. Published by Elsevier Ltd. All rights reserved.

1. Introduction

Diabetes mellitus is one of the most prevalent chronic diseases world wide. Impaired wound healing is a complication of diabetes that results in a failure diabetic foot ulcers (DFUs) to completely heal [1]. Complications of DFUs lead to frequent hospitalization and, in extreme cases, to amputation, resulting in high hospital costs and a poor quality of life for patients [2]. DFUs are a multifactorial complication that result particularly as a consequence of peripheral neuropathy, impaired vascular function, impaired angiogenesis and/or chronic inflammation [1,3].

Recently it became evident that the peripheral nerves and cutaneous neurobiology contribute to wound healing [4]. Loss of peripheral sensory and autonomic nerves reduces the production of neuropeptides that are important for proper wound healing

[3]. Neurotensin (NT) is a bioactive neuropeptide that is widely distributed in the brain and in several peripheral tissues [5,6]. NT interacts with leukocytes, mast cells, dendritic cells and macrophages, leading to cytokine release and chemotaxis, which can modulate the immune response. In addition, NT affects microvascular tone, vessel permeability, vasodilation/vasoconstriction and new vessel formation, helping to improve angiogenesis during wound healing [3,7,8].

Some studies have demonstrated that topical application of neuropeptides, such as substance P and neuropeptide Y, can improve wound healing in diabetes [9,10]. However, the major problem with topical administration of peptides is their short half-life and loss of bioactivity in the peptidase-rich wound environment [11]. An alternative strategy to overcome this problem is the use of biocompatible wound dressings for the sustained delivery of neuropeptides. These dressings should, however, also replicate the characteristics of skin in order to promote the proliferation and migration of fibroblasts and keratinocytes, as well as to enhance collagen synthesis, leading to proper healing with little scar formation [12,13].

Wound dressings based on natural polymers have been extensively applied to simulate extracellular matrix (ECM) regeneration

---

after injury [12,13]. One of the most used naturally based polymers for wound healing applications is chitosan [12], which is a linear co-polymer of D-glucosamine and N-acetyl-D-glucosamine [14]. Since it is derived from chitin, a polymer found in fungal cell walls and the crustacean exoskeleton, it is a relatively inexpensive and abundant material [15]. In addition, it has proven to be biodegradable, biocompatible, non-antigenic, non-toxic, bioadhesive, antimicrobial, bioactive and to have hemostatic capacity [15–17]. Furthermore, chitosan promotes tissue granulation and accelerates wound healing through the recruitment of inflammatory cells such as polymorphonuclear leukocytes (PMN) and macrophages to the wound site [18].

To increase its poor solubility in water chitosan functional groups can be chemically modified to produce water-soluble chitosan derivatives such as N-carboxymethyl chitosan (CMC), 5-methyl pyrrolidinone chitosan (MPC) and N-succinyl chitosan (SC) [19–21]. These chitosan derivatives are functional biomaterials that maintain the antibacterial and non-cytotoxic properties of the parent chitosan. In addition, they stimulate the extracellular lysozyme activity of skin fibroblasts [22,23].

The aim of this study was to develop and apply wound dressings prepared from the chitosan derivatives referred above (CMC, MPC, SC) for the prolonged and efficient delivery of NT to diabetic and non-diabetic wounds, while also conferring wound protection and comfort. The progression of skin wound healing in diabetic and non-diabetic mice was also evaluated by analysis of the inflammatory and angiogenic effects of NT when applied to skin wounds alone or loaded into MPC-based dressings.

2. Materials and methods

2.1. Materials

Chitosan (medium molecular weight, 90% degree of acetylation confirmed by ^{1}H NMR), glyoxylic acid monohydrate (98%), sodium hydroxide, sodium borohydride (99.5%), levulinic acid (98%), succinic anhydride (97%), reduced glutathione (GSH), 5,5′-dithio-bis(2-nitrobenzoic acid) (DTNB), dialysis membranes (Spectra/Por 6) with a MWCO of 8000 Da and methanol p.a. were obtained from Sigma–Aldrich (USA). Acetic acid was obtained from Panreac (Spain), and ethanol was purchased from Riedel-de-Haen (Germany). Ketamine (Clorketam 1000) was obtained from Vétoquinol (Portugal) and xylazine (Rompun) from Bayer HealthCare (Germany). NT was purchased from Bachem (Switzerland). The antibodies against tumor necrosis factor-α (TNF-α) and metalloproteinase 9 (MMP-9) were purchased from Cell Signaling Technology (USA) and the antibodies against vascular endothelial growth factor (VEGF) and actin were purchased from the Millipore Corp. (USA).

2.2. Synthesis of the chitosan derivatives CMC, MPC and SC

Chitosan (2 g) was reacted with glyoxylic acid (1.16 g), levulinic acid (5 ml) or succinic anhydride (3 g) to synthesize CMC, MPC and SC, respectively [24,25], following by precipitation with ethanol and dialysis to remove unreacted reagents. Foams of CMC, MPC and SC were prepared by freeze-drying, adding 1.5 ml of each solution to 12-well plates. The average thickness of the materials obtained was 250 ± 15 μm. All samples were stored at −20 °C, away from light and humidity, before use. The degree of substitution of each of the derivatives was calculated by ^{1}H NMR using a Bruker Avance III 400 MHz spectrometer with a 5 mm TIX triple resonance detection probe using D_2O acidified with acetic acid (10 μl of acetic acid in 600 μl of D_2O).

2.3. Scanning electron microscopy (SEM)

SEM micrographs were obtained at 5 keV (JEOL model JSM-5310, Japan). Samples were coated with gold (approximately 300 Å) in an argon atmosphere.

2.4. Water vapor and water sorption capacities

Samples of CMC, MPC and SC, 22 mm in diameter, were dried at 37 °C for 72 h until a constant weight was achieved. Both water vapor and water sorption capacities were measured gravimetrically. In the first case dried foams were exposed to a 95% relative humidity atmosphere, in a desiccator containing a saturated solution of potassium sulfate at 32 °C according to Dias et al. [26]. In the second case samples were immersed into phosphate buffer (pH 7) at 37 °C and weighed after removing the surface phosphate buffer using filter paper.

Samples were weighed at fixed time intervals until they reached equilibrium. The water vapor and water sorption capacities were calculated as the ratio between the sample weight at time t and the initial sample dry weight. All samples were measured in duplicate.

2.5. In vitro release kinetics

Kinetic release profiles of GSH were determined spectrophotometrically (Jasco model 630, Japan) at 412 nm. Known amounts of GSH solution (5 mM) were loaded into previously weighed samples of each polymer. The GSH solution had been previously placed in an ultrasonic bath to prevent oxidation. After drying the samples were immersed in phosphate buffer at pH 6, 7 or 8 at 32 °C with orbital stirring (100 r.p.m.) for 8 h. The quantification of GSH release was based on the Ellman's test. This test is based on the addition of DTNB, a yellow water-soluble compound that reacts with free sulfhydryl groups in peptide solutions. At predetermined time points an aliquot (100 μl) of the released solution was removed and analyzed using a mixture of 1800 μl of phosphate buffer and 100 μl of DNTB stock solution (20 mM). 100 μl of fresh phosphate buffer was added to the medium each time point. Each sample was analyzed in duplicate.

2.6. Cell culture

Mouse leukemic monocyte macrophages (Raw 264.7) and human keratinocyte (HaCaT) cells were cultured in DMEM (Dulbecco's modified Eagle's medium), pH 7.4, supplemented with 10% heat-inactivated fetal bovine serum (FBS), 3.02 g l^{-1} sodium bicarbonate, 30 mM glucose, 100 U ml^{-1} penicillin, 100 μg ml^{-1} streptomycin at 37 °C in a humidified incubator containing 5% CO_2. Sub-culturing was performed according to ATCC recommendations. The Raw 264.7 and HaCaT cell lines were purchased from the ATCC (No. TIB-71) and CLS (No. 300493), respectively.

2.7. MTT assay

Raw 264.7 (8×10^4 cells per well) and HaCaT (4×10^4 cells per well) cells were plated individually in 12-well plates with 430 μl of DMEM above the previously sterilized (UV light for at least 30 min) biomaterials. After 24 and 48 h incubation 43 μl of 3-(4,5-dimethylthiazol-2-yl)-2,5-diphenyltetrazolium bromide (MTT) solution (5 mg ml^{-1}) was added to each well. The plates were further incubated at 37 °C for 1 h in a humidified incubator containing 5% CO_2. After this period 300 μl of acidic isopropanol (0.04 N HCl in isopropanol) was added. Quantification was performed using an ELISA automatic microplate reader (SLT, Austria) at 570 nm, with a

reference wavelength of 620 nm. Each sample was analyzed in duplicate.

2.8. NO production (Griess method)

Raw 264.7 (8×10^4 cells per well) cells were plated in 12-well plates with 430 μl of DMEM above the previously sterilized (UV light for at least 30 min) biomaterials. After 24 and 48 h incubation 170 μl of the supernatant was mixed with an equal volume of Griess reagent (1% sulfanilamide, 0.1% N-1-naphthelenediamine dihydrochloride in 2.5% phosphoric acid). After 30 min incubation in the dark the absorbance was measured at 550 nm in a microplate reader (SLT, Austria). Nitrite concentration was calculated from a previously obtained nitrite standard curve.

2.9. In vivo wound closure

We used male C57BL/6 mice (Charles River Corp. Inc., Barcelona, Spain) weighing 25–30 g. The animals were maintained at normal room temperature (22–24 °C) on a 12 h light/dark cycle, with free access to a commercial pellet diet and water. After the wound procedure, the animals were kept in individual cages. All experiments were conducted according to the National and European Communities Council directives on animal care.

Diabetes was induced by a single intraperitoneal injection of streptozotocin (STZ) (150 mg kg^{-1}) in citrate buffer, pH 4.5. 4 days after diabetes induction blood glucose levels were checked using an Accu-Chek Aviva glucometer (Roche Diagnostics GmbH, Germany). Animals with blood glucose levels higher than 300 mg dl^{-1} were considered diabetic. Mice were anesthetized by intraperitoneal injection of xylazine (13 mg kg^{-1}) and ketamine (66.7 mg kg^{-1}). The dorsal hair of control and diabetic mice was shaved and two 6 mm diameter full thickness wounds were created with a biopsy punch.

C57BL/6 mice were randomly divided into six treatment groups of control (non-diabetic) and diabetic mice, three groups for day 3 (I, II, III) and three similar groups for day 10 (IV, V, VI). Groups I and IV were treated with MPC dressings alone (6–12 animals), groups II and V with topical application of 50 μg ml^{-1} NT (7 animals) and groups III and VI with 50 μg ml^{-1} NT-loaded MPC dressings (7–9 animals).

For each animal one of the wounds served as a control (PBS application only), while the other received treatment. The dried MPC foams were applied over the wounds and wetted with 5 μl of PBS or NT solution (50 μg ml^{-1}) to produce hydrogels with improved adherence and mucoadhesive capacities. By visual inspection it was possible to observe that the dressings persisted over the wound until approximately day 6–7. The progress of wound healing was evaluated periodically by acetate tracing until day 10. Topical application of PBS or NT (alone or loaded into prepared MPC dressings) was performed daily. On day 3 or 10 C57BL/6 mice were killed and around 2 mm of tissue and skin surrounding the wound were harvested. These time points were chosen to evaluate the inflammatory (day 3) and the proliferation/remodeling (day 10) phases of wound healing.

2.10. Real time reverse transcription polymerase chain reaction (RT-PCR)

Total RNA was isolated from skin with a RNeasy Mini Kit according to the manufacturer's instructions (Qiagen, USA). First strand cDNA was synthesized using high capacity cDNA reverse transcription. Then, real time RT-PCR was performed in a BioRad MyCycler iQ5. Primer sequences will be given upon request. Gene expression changes were analyzed using iQ5Optical system software v2. The results were normalized using a housekeeping gene,

TATA box binding protein (TBP), which was previously validated in our laboratory. Quantitative RT-PCR results were analyzed through ΔC_t calculations.

2.11. Western blotting

Skin tissue lysate was homogenized in RIPA buffer (50 mM Tris–HCl, pH 8, 150 mM NaCl, 1% NP-40, 0.5% sodium deoxycholate, 0.1% sodium dodecyl sulfate, 2 mM EDTA, protease inhibitor cocktail, phosphatase inhibitor cocktail and 1 mM dithiothreitol). Protein concentration was determined using the bovine serum albumin (BSA) method. The skin lysates were denatured at 95 °C for 5 min in sample buffer. 40 μg of total protein were resolved by 12% SDS–PAGE and transferred to PVDF membranes. The membranes were blocked with 5% fat-free dry milk in Tris-buffered saline containing 0.1 vol.% Tween 20 (TBS-T) for 1 h at room temperature. After blocking the membranes were incubated with primary antibodies against the TNF-α (1:500), VEGF (1:1000) and MMP-9 (1:500), overnight at 4 °C. After incubation the membranes were washed and incubated for 1 h at room temperature with anti-rabbit antibody (1:5000) or anti-mouse antibody (1:5000). The membranes were exposed to ECF™ reagent followed by scanning in a VersaDoc (Bio-Rad Laboratories, Portugal). For normalization the membranes were re-probed with an anti-actin antibody (1:10000). The generated signals were analyzed using Image-Quant TL software.

2.12. Hydroxyproline content

This analysis was performed using a Hydroxyproline Assay Kit (Sigma Aldrich, USA). Briefly, 10 mg of skin tissue were homogenized in 100 μl of water and hydrolyzed with 12 M HCl at 120 °C for 3 h. 25 μl of the supernatant were transferred to a 96-well plate and evaporated in an incubator at 60 °C until totally dry. Then 100 μl of chloramine T/oxidation buffer and 100 μl of diluted DMAB Reagent were added to each sample and incubated for 90 min at 60 °C. Quantification was performed using an ELISA automatic microplate reader (SLT, Austria) at 560 nm.

2.13. Histopathological analysis

For histological preparation the skin was fixed in 10% neutral buffered formalin and then embedded in paraffin. Skin tissue was sectioned into 3 μm thickness slices for histopathological examination by hematoxylin/eosin (H&E) staining and for collagen formation by Masson's trichrome staining, using standard procedures. The stained sections were observed with a Nikon H600L microscope with a DXM 1200F digital camera (Nikon, Germany). Analysis of stained skin sections was performed by an experienced pathologist.

2.14. Statistical analysis

Results are expressed as means ± SEM (Structural Equation Modeling). Statistical analysis was performed using one-way ANOVA followed by Tukey's multiple comparison tests or through an unpaired or paired *t*-test using GraphPad Prism (GraphPad Software Inc., USA). *P* values lower than 0.05 were considered statistically significant.

3. Results

3.1. Degree of substitution and morphology of CMC, MPC and SC

The degree of substitution (number of native chitosan amino groups substituted) of each chitosan derivative was confirmed by

^{1}H NMR as 25.5%, 24% and 28.5% for CMC, MPC and SC, respectively (Supplementary Fig. S1). The schematic representation of each derivative is shown in Fig. 1A.

The different morphologies obtained for each of the prepared chitosan derivative foams are shown in Fig. 1B. CMC presents a honeycomb-like porous structure, with larger pores than MPC and SC, which presented an interlaced fiber-like pattern. The fiber-like structure of SC seems to be thinner than the one observed for MPC.

3.2. Water vapor and water swelling properties

Fig. 2A shows the water vapor sorption behavior of the CMC, MPC and SC foams under controlled humidity (95%) and temperature conditions (32 °C). The data show that the hydrophilicity of the materials changes in the sequence SC > MPC > CMC. All the samples achieved equilibrium after approximately 8 h. At this point SC had adsorbed 35% of its initial weight as water vapor, while MPC and CMC adsorbed 24% and 14%, respectively.

In terms of water swelling capacity, Fig. 2B shows that SC had the fastest swelling rate, reaching a maximum (2438%) after 5 h, after which it starts to decrease. CMC had the lowest swelling capacity (163%), while MPC had an intermediate water swelling profile. Both the MPC and SC foams reached water swelling equilibrium after approximately 6 h and both maintained their structure (macroscopically, to the naked eye) until day 15 under the experimental conditions.

3.3. In vitro release kinetics

GSH was used as a model peptide molecule for in vitro release kinetics studies. The release of GSH from CMC, MPC and SC foams was followed for a period of 8 h at three different pH values (pH 6, 7 and 8), which is the pH range observed during the wound healing process. The release profiles measured for each chitosan derivative at pH 7 are presented in Fig. 3. Data measured at pH 6 and 8 are presented as Supplementary data (Supplementary Fig. S2) due to the similarities observed at the different pH values studied in this work. The release profiles show that equilibrium was attained between 5 and 8 h for all the samples and that the amount of GSH released from SC was significantly higher than from CMC and MPC (~9 and 4 times higher, respectively). When comparing the amount of GSH released after 8 h with the total GSH loaded the results show that ~50% was released from CMC and MPC, while almost 100% was released from SC. The results also show that the amount of GSH released from the chitosan derivatives was not significantly affected over the pH range studied and, considering the experimental error, averaged 32.33 ± 0.72%, 67.65 ± 6.77% and 287.18 ± 14.92% GSH released (%) per $m_{polymer}$ (g) for CMC, MPC and SC, respectively.

### 3.4. In vitro biocompatibility of CMC and MPC

There was no significant difference in the viability of Raw and HaCaT cells exposed to the CMC and MPC foams for 24, 48 and 72 h, compared with the control, as shown in Fig. 4A and B, respectively. NO is produced by macrophages in response to an inflammatory stimulus. The production of nitrites, with the final stable breakdown product NO, measured after exposure of the cells to the chitosan derivatives (Fig. 4C) was also not significantly affected, however, a slight increase in nitrite produced was observed after 72 h, which may be due to the stress which cells are subjected to after this exposure period.

3.5. Wound healing in vivo

Fig. 5 shows the effects of the different topical treatments studied in this work: NT alone, MPC foam alone and NT-loaded MPC foam in both control (Fig. 5A) and diabetic (Fig. 5B) mice. PBS served as a control. All treatments were shown to significantly reduce the wound area, compared with PBS-treated wounds, in both control and diabetic mice. NT alone significantly reduced the
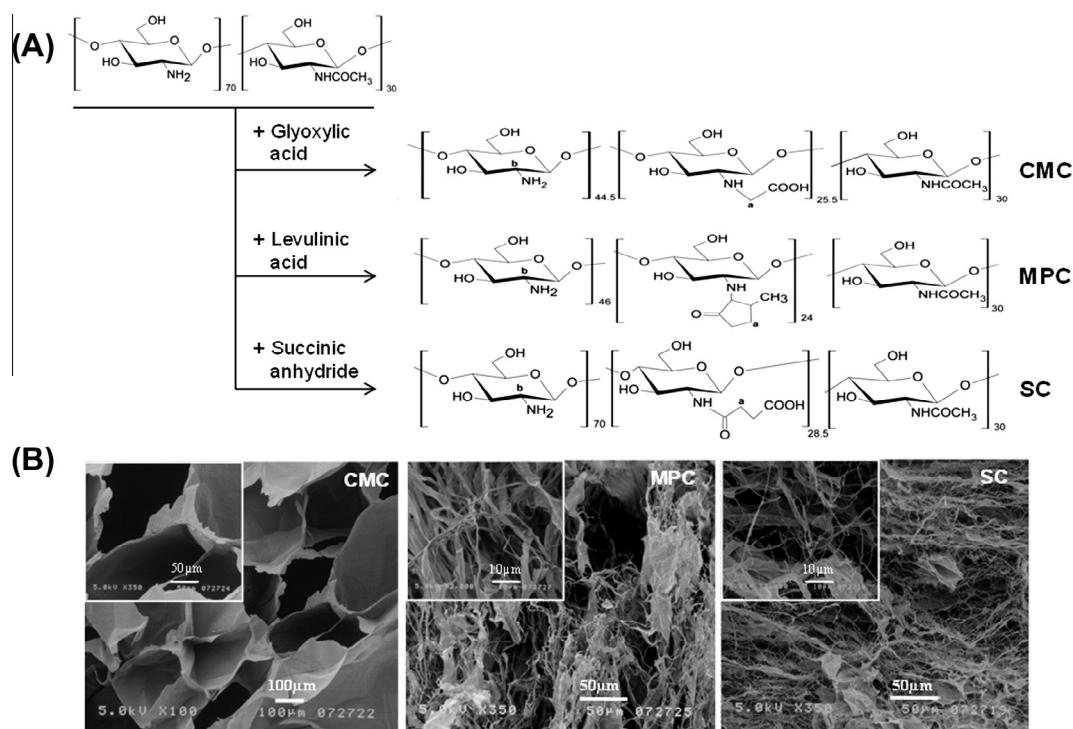
Fig. 1. (A) Chemical synthesis of the chitosan derivatives: N-carboxymethyl chitosan (CMC), 5-methyl pyrrolidinone chitosan (MPC) and N-succinyl chitosan (SC). (B) SEM micrographs of the non-loaded chitosan derivatives CMC, MPC and SC representing the different structures obtained by freeze-drying. The inserts are at higher magnification.
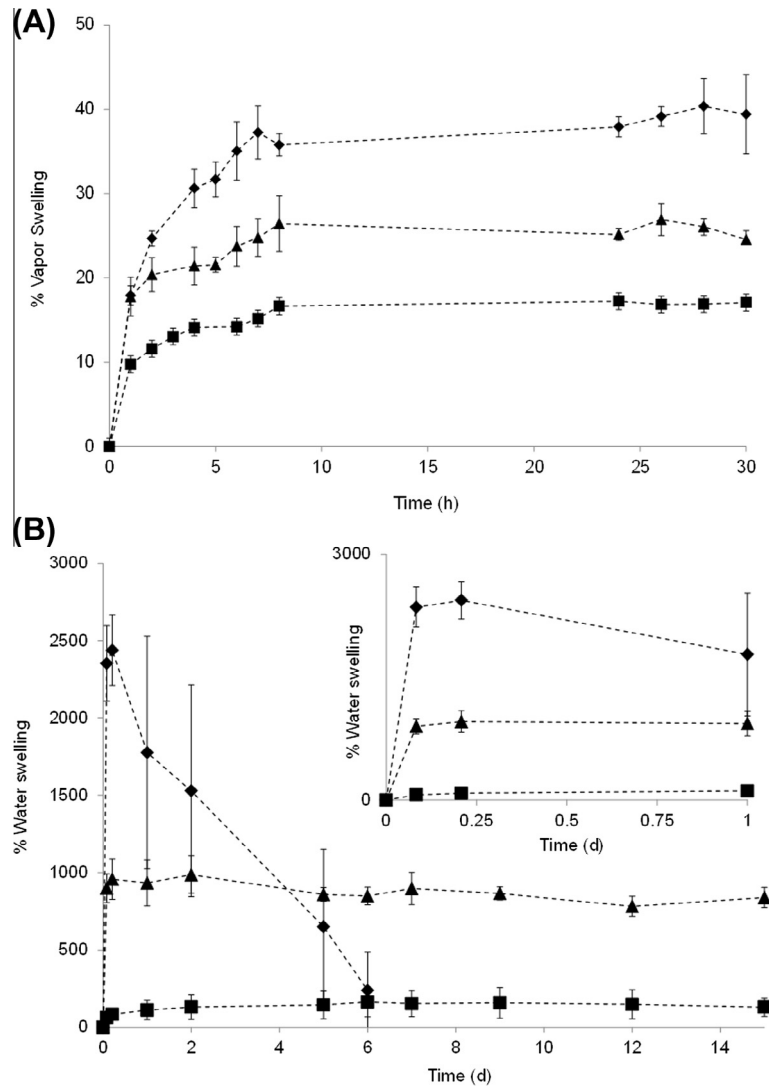
Fig. 2. (A) Water vapor and (B) water swelling profiles for the CMC (■), MPC (▲) and SC (♦) foams. The insert represents a magnification of the water swelling profiles for day 1. The lines serve only as guides for the eye. The results are presented as means ± SEM of two independent experiments.
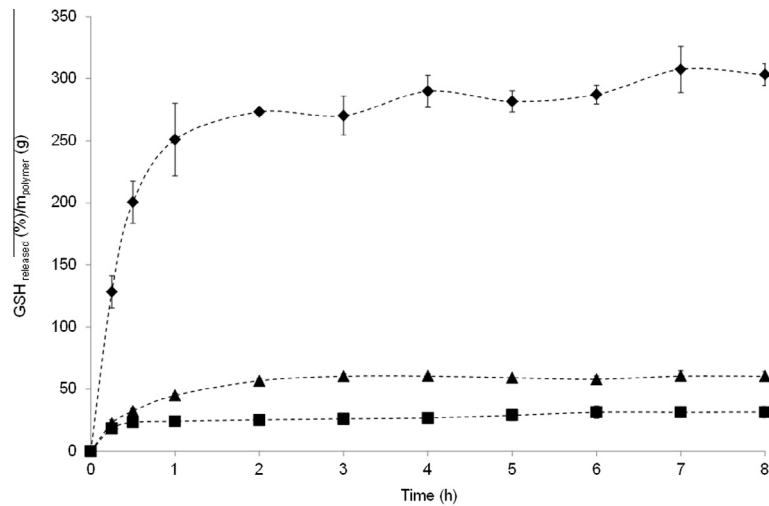
Fig. 3. Release kinetic profiles for GSH from the CMC (■), MPC (▲) and SC (♦) foams at pH 7 measured for 8 h at 37 °C. The lines serve only as guides for the eye. The results are presented as means ± SEM of two independent experiments.

wound size in control mice 3 days post-wounding, by 22% ($P < 0.05$), compared with PBS-treated wounds (Fig. 5A). In diabetic mice the wound size of the NT-treated wounds was also significantly reduced on days 3 and 5, by 29% ($P < 0.01$) and 34%
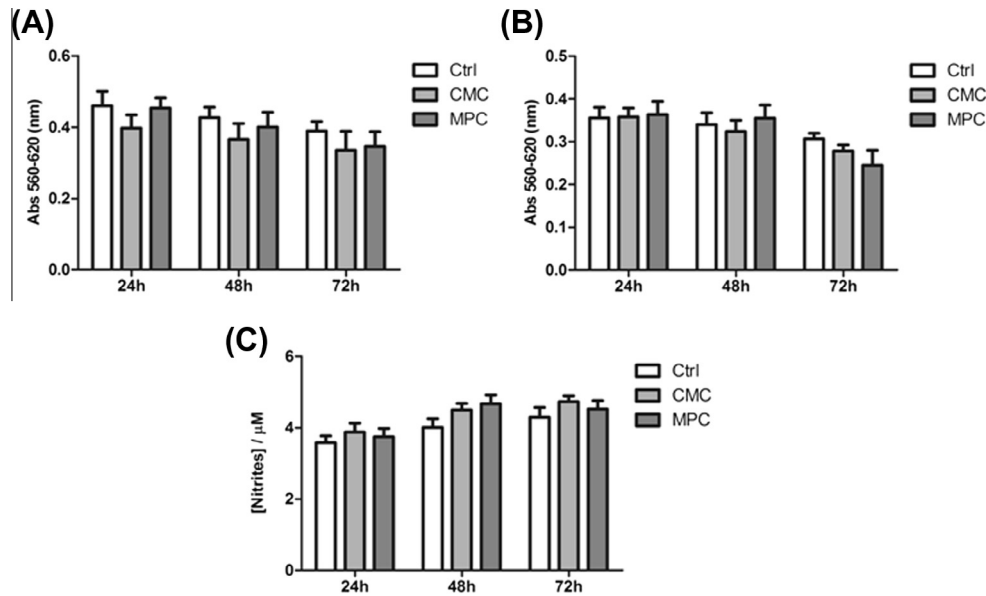
Fig. 4. Cell viability of (A) Raw and (B) HaCaT cells in the presence of CMC or MPC foams for 24, 48 and 72 h. (C) NO production in Raw cells. The results are presented as means ± SEM of three independent experiments.

($P < 0.01$), respectively. A different healing profile was observed for the non-loaded and NT-loaded MPC-treated wounds in both the control and diabetic mice. A significant decrease in wound area was evident on day 1 post-wounding with non-loaded MPC (48%, $P < 0.001$) and NT-loaded MPC (43%, $p < 0.001$), compared with PBS-treated wounds (Fig. 5A). In diabetic animals the profile of wound closure was similar, however, the NT-loaded MPC

treatment was significantly more effective than MPC alone, with a wound reduction of 50% ($P < 0.001$) rather than 35% ($P < 0.001$) for the non-loaded dressing (Fig. 5B).

3.6. Cytokine, MMP-9, collagen and growth factor expression at the wound site

In order to address the pattern of cytokine gene expression in untreated and treated wounds 0, 3 and 10 days post-wounding the gene expression of inflammatory cytokines (TNF-α, interleukin (IL)-6, IL-8 and IL-1β) and several types of collagen (COL1A1, COL1A2 and COL3A1) were measured. The results are presented in Fig. 6A–N. Other important factors, such as MMP-9 and the growth factors endothelial growth factor (EGF), VEGF and platelet-derived growth factor (PDGF), transforming growth factor (TGF)β1 and TGFβ3 were also evaluated. Their expression is presented in Supplementary Fig. S3.

In unwounded skin (day 0, baseline) all the measured inflammatory cytokines were significantly increased in the skin of diabetic animals compared with the healthy controls (Fig. 6A–G). On the other hand, all types of collagens analyzed were significantly reduced ($P < 0.001$) (Fig. 6I–N).

We observed a significant increase in the inflammatory stimulus on day 3 post-wounding , as one might expect, compared with day 0 controls. However, the same effect was not observed in diabetic mice.

Furthermore, in control mice on day 3 MPC treatment alone significantly reduced the expression of TNF-α ($P < 0.05$), IL-6 ($P < 0.05$) and IL-1β ($P < 0.05$), while NT alone decreased the expression of TNF-α ($P < 0.05$) and IL-1β ($P < 0.05$) (Fig. 6A, C and G, respectively). NT-loaded MPC treatment reduced TNF-α expression ($P < 0.05$), however, IL-6 and IL-8 expression were significantly increased in the controls ($P < 0.05$). In diabetic mice TNF-α expression was significantly higher for all treatments ($P < 0.05$), but IL-1β expression was reduced upon NT-loaded MPC treatment ($P < 0.05$) compared with PBS alone.

On day 3 NT alone reduced EGF expression in diabetic mice ($P < 0.05$) and increased VEGF expression ($P < 0.05$) in the control (Supplementary Fig. S3C and E). In addition, while NT and the NT-loaded MPC foam significantly induced TGFβ3 expression
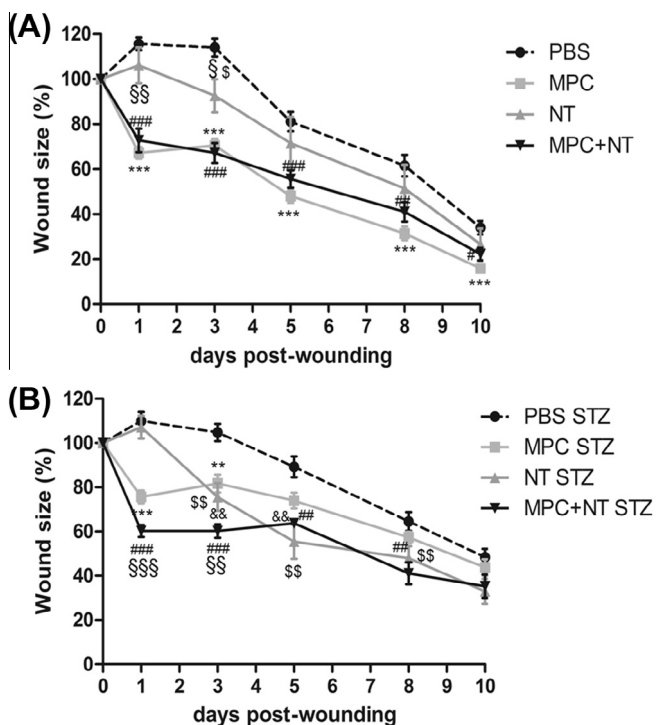
Fig. 5. Wound size measurements for the MPC, NT and NT-loaded MPC foam treatments in (A) control and (B) diabetic mice. The wound size was determined on days 0, 1, 3, 5, 8 and 10 post-wounding. The results are presented as means ± SEM of 7–18 independent experiments. **$P < 0.01$ MPC compared with PBS, ***$P < 0.001$ MPC compared with PBS, ##$P < 0.01$ MPC + NT compared with PBS, ###$P < 0.001$ MPC + NT compared with PBS, $^{\$\$}P < 0.01$ NT compared with PBS, $^{\$\$\$}P < 0.001$ NT compared with MPC + NT, $^{\&\&}P < 0.01$ MPC compared with MPC + NT.
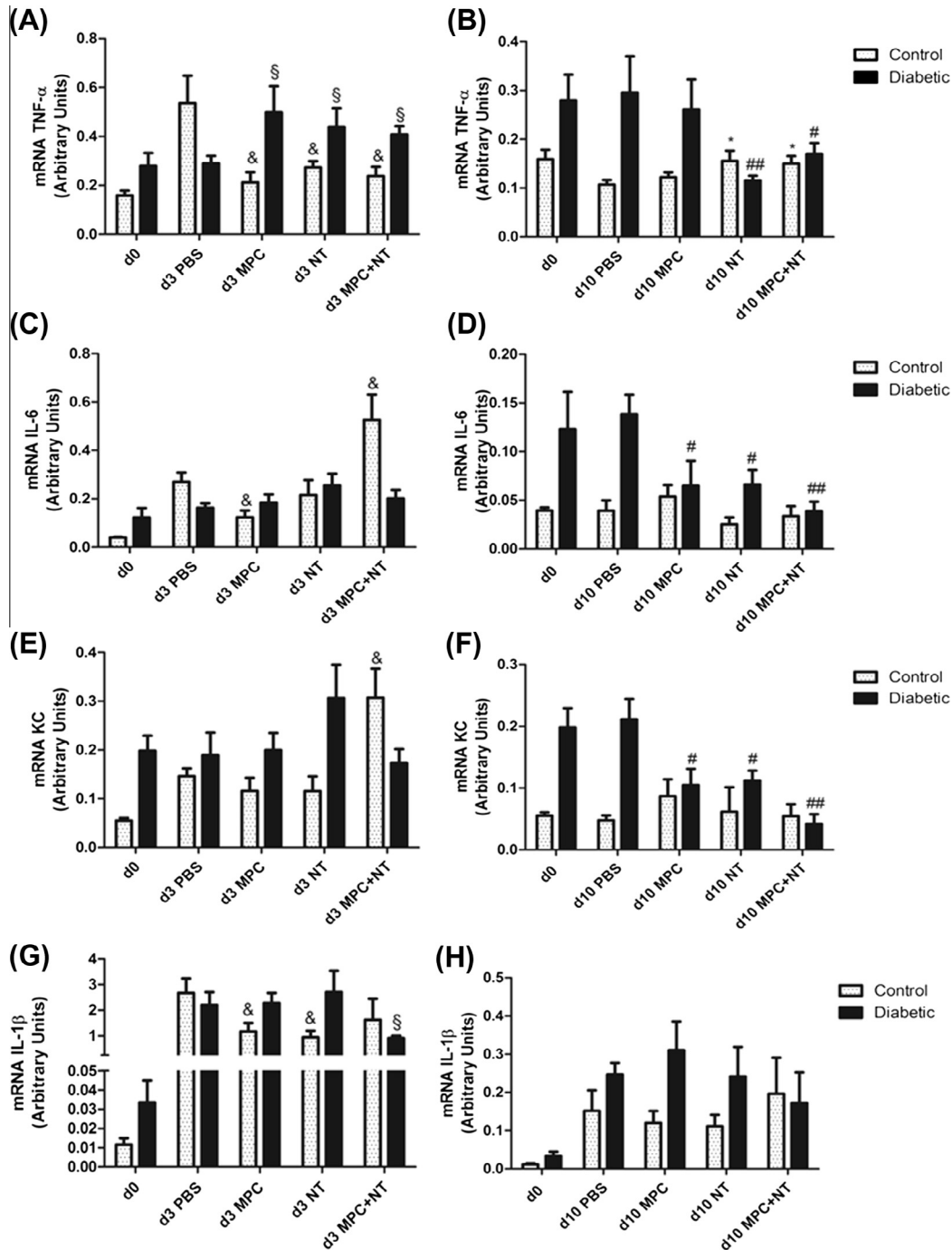
Fig. 6. Gene expression profiles for (A, B) TNF-α, (C, D) IL-6, (E, F) IL-8, (G, H) IL-1β, (I, J) COL1A1, (K, L) COL1A2 and (M, N) COL3A1 in skin biopsies before and after treatment, on days 3 (A, C, E, G, I, K, M) and 10 (B, D, F, H, J, L, N) post-wounding. The results are presented as means ± SEM of 7–18 independent experiments. $^{\&}P < 0.05$ compared with control PBS day 3, $^{*}P < 0.05$ compared with PBS day 10, $^{**}P < 0.01$ compared with PBS day 10, $^{\S}P < 0.05$ compared with diabetic PBS day 3, $^{\#}P < 0.05$ compared with diabetic PBS day 10, $^{\#\#}P < 0.01$ compared with diabetic PBS day 10.

($P < 0.001$) in controls, no differences were observed in diabetic skin (Supplementary Fig. S3K). Collagen genes showed higher expression in control skin, and NT treatment significantly increased COL1A1, COL1A2 and COL3A1 expression in diabetic skin (Fig. 6I, K and M, respectively).

On day 10 the expression of all inflammatory cytokines was diminished to baseline levels in the controls with the exception of TNF-α, which increased ($P < 0.05$) on NT and NT-loaded MPC application, compared with PBS-treated wounds. In diabetic mice all treatments reduced the expression of TNF-α, IL-6 and IL-8

($P < 0.05$ in all cases) (Fig. 6B, D and F, respectively). The non-loaded and NT-loaded MPC treatments caused a decrease in MMP-9 expression in both control and diabetic mice ($P < 0.05$) (Supplementary Fig. S3B). In addition, the NT-loaded MPC treatment reduced EGF in diabetic mouse skin ($P < 0.05$) (Supplementary Fig. S3D).

NT and the NT-loaded MPC foam significantly induced TGFβ1 and TGFβ3 expression ($P < 0.001$) in controls on day 10, but no differences were observed in diabetic skin. In diabetic skin only NT treatment significantly reduced TGFβ3 ($P < 0.05$) (Supplementary
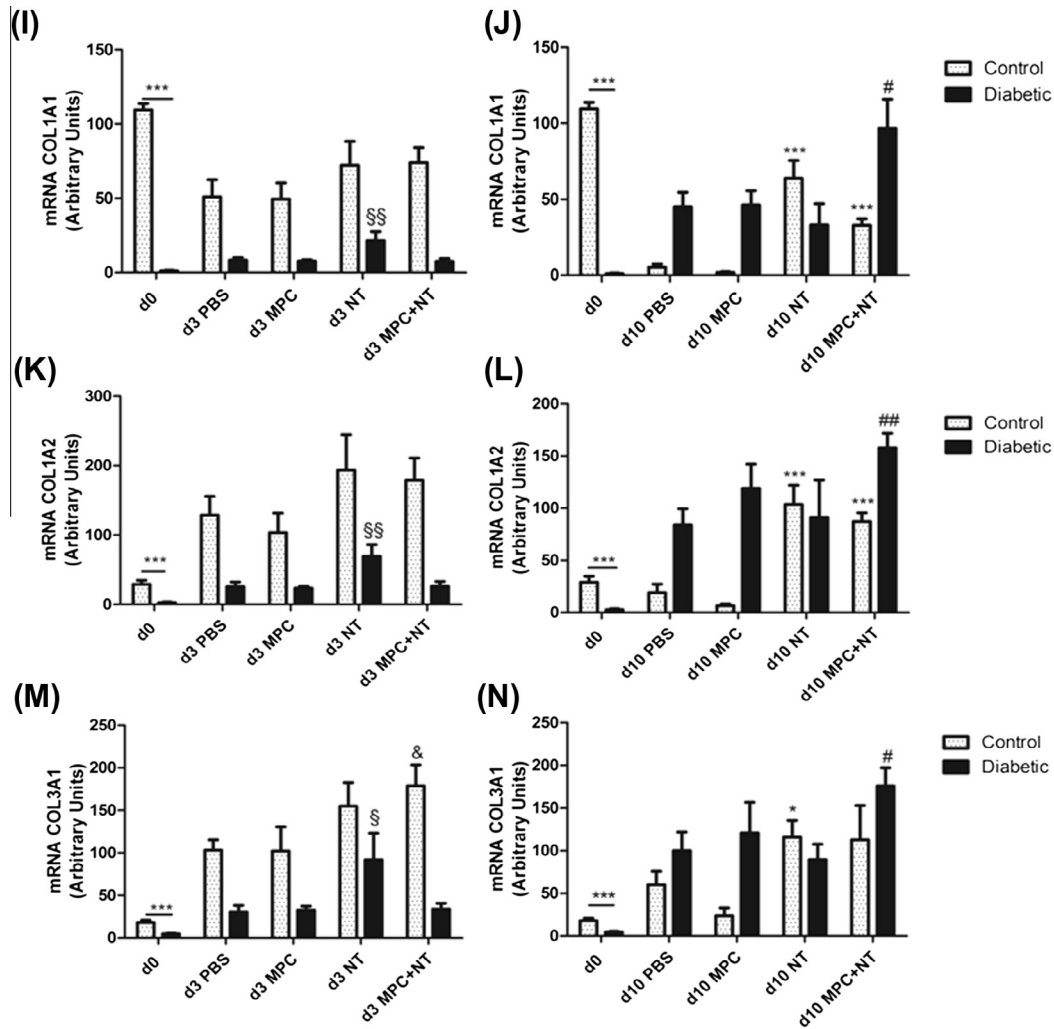
Fig. 6 (*continued*)

Fig. S3J and L). In addition, NT and the NT-loaded MPC foam stimulated an increase in COL1A1 and COL1A2 ($P < 0.001$) in control mice, while in diabetic mice only NT-loaded MPC significantly induced expression of all collagen genes (Fig. 6J, L and N).

3.7. Protein expression at the wound site

Western blot analysis of skin tissue was performed to evaluate protein expression levels at the wound site (Fig. 7). On day 0 only MMP-9 was significantly increased ($P < 0.001$) in diabetic mice compared with controls. On day 3 NT treatment induced a reduction in MMP-9 protein levels in control mice. MPC treatment increased the TNF-α level at diabetic wound site. In contrast, NT and the NT-loaded MPC foam significantly reduced MMP-9 ($P < 0.05$) and TNF-α ($P < 0.001$) protein levels.

On day 10 MPC, NT and NT-loaded MPC treatment significantly reduced MMP-9 protein expression compared with PBS treatment, in both control and diabetic skin. TNF-α protein expression was not detected by Western blot on day 10 after all treatments.

3.8. Hydroxyproline content at the wound site

To evaluate collagen deposition in mouse skin hydroxyproline levels were measured in unwounded and wounded (treated and non-treated) skin (Fig. 8). In unwounded skin hydroxyproline levels were significantly decreased ($P < 0.01$) in diabetic mice compared with control skin. On day 3 post-wounding NT significantly increased ($P < 0.05$) hydroxyproline content in diabetic skin, while on day 10 this effect was observed with NT-loaded MPC in control and diabetic skin ($P < 0.05$ and $P < 0.01$), respectively.

3.9. Histopathological analysis of the wound

For histopathological analysis of control and diabetic skin tissue we used H&E and Masson's trichrome staining (Fig. 9A and B, respectively). In unwounded skin an increase in epidermis skin thickness was evident in diabetic mice compared with controls. On day 3 post-wounding all the treatments stimulated an increase in epidermis thickness, which was more significant for the non-loaded and NT-loaded MPC treatments in diabetic skin (Table 1). On day 10 the epidermis thickness profile was similar, with a stronger effect in diabetic skin (Fig. 9A and Table 2). Specific re-epithelialization profiles were observed: in control mice re-epithelialization occurred from the bottom to top with basal cells in the epidermis covering the scar; in diabetic mice re-epithelialization occurred over the granulation inflammatory tissue while this was undergoing repair, without correlation with the applied treatments, in both groups (Tables 2 and 3).
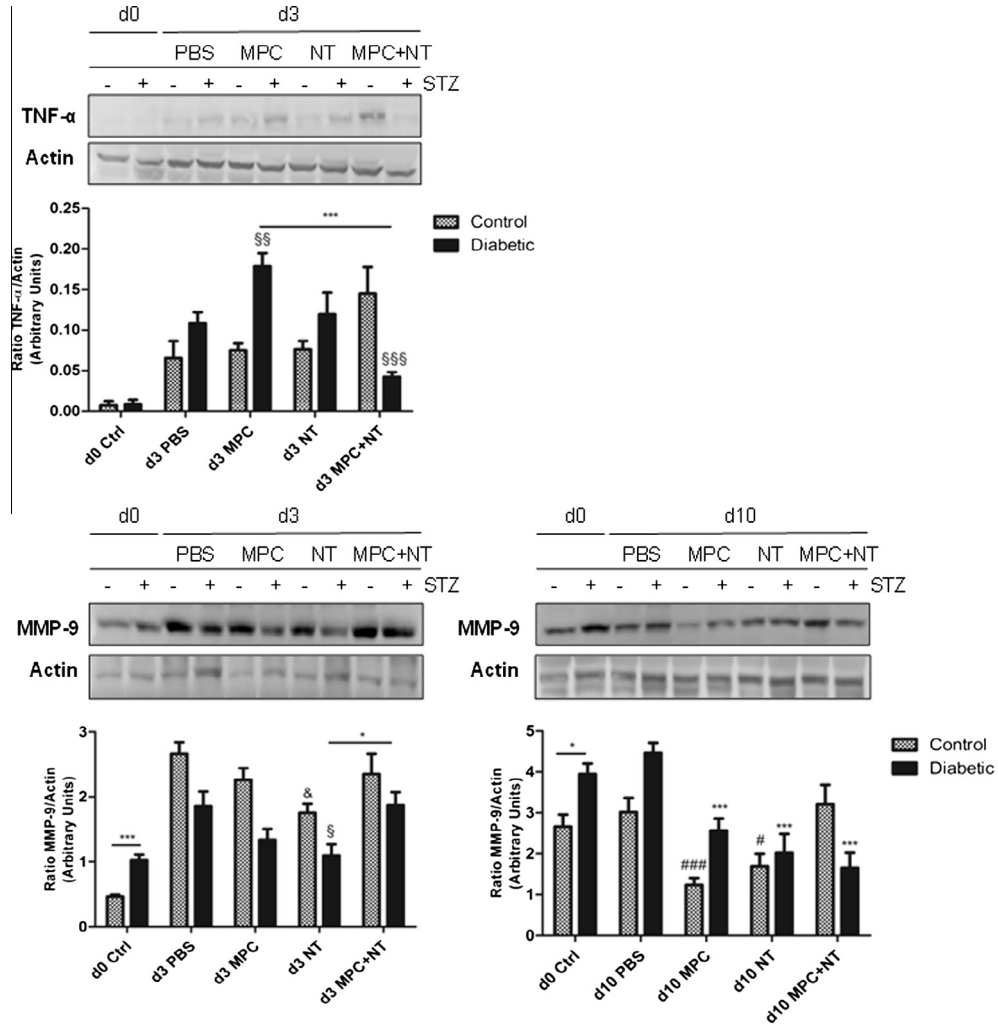
Fig. 7. Expression of TNF-α and MMP-9 protein in unwounded skin (day 0) and after treatment, on days 3 and 10 post-wounding. The results are presented as means ± SEM of 3–5 independent experiments. [&]$P < 0.05$ compared with control PBS day 3, [*]$P < 0.05$ compared with diabetic PBS day 10, [***]$P < 0.001$ compared with diabetic PBS day 10, [§]$P < 0.05$ compared with diabetic PBS day 3, [§§]$P < 0.01$ compared with diabetic PBS day 3, [#]$P < 0.05$ compared with control PBS day 10, [##]$P < 0.01$ compared with control PBS day 10.
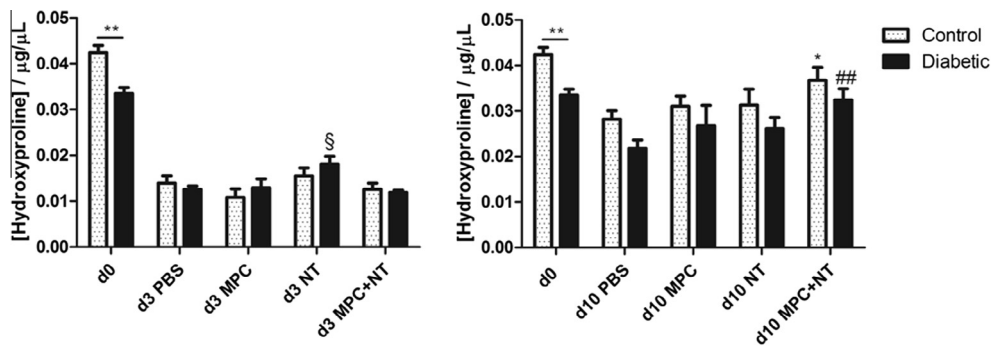
Fig. 8. Hydroxyproline content in unwounded skin (day 0) and after treatment, on days 3 and 10 post-wounding. The results are presented as means ± SEM of 4–6 independent experiments. [*]$P < 0.05$ compared with PBS day 10, [§]$P < 0.05$ compared with diabetic PBS day 3, [##]$P < 0.01$ compared with diabetic PBS day 10.

On day 3 neither MPC, NT alone or NT-loaded MPC treatment affected the number of polymorphonuclear leukocytes (PMN) and lymphocytes in control skin, however, in diabetic skin fewer of these inflammatory cells were recruited to the wound site compared with PBS treatment. In addition, there was higher production of fibrin in diabetic skin, while no plasma cells were observed in either control or diabetic skin (Table 3). On day 10 there was no significant recruitment of PMN and lymphocytes observed in control skin, while in diabetic wounds treated with either MPC, NT alone or NT-loaded MPC PMN cells, lymphocytes and plasma cells
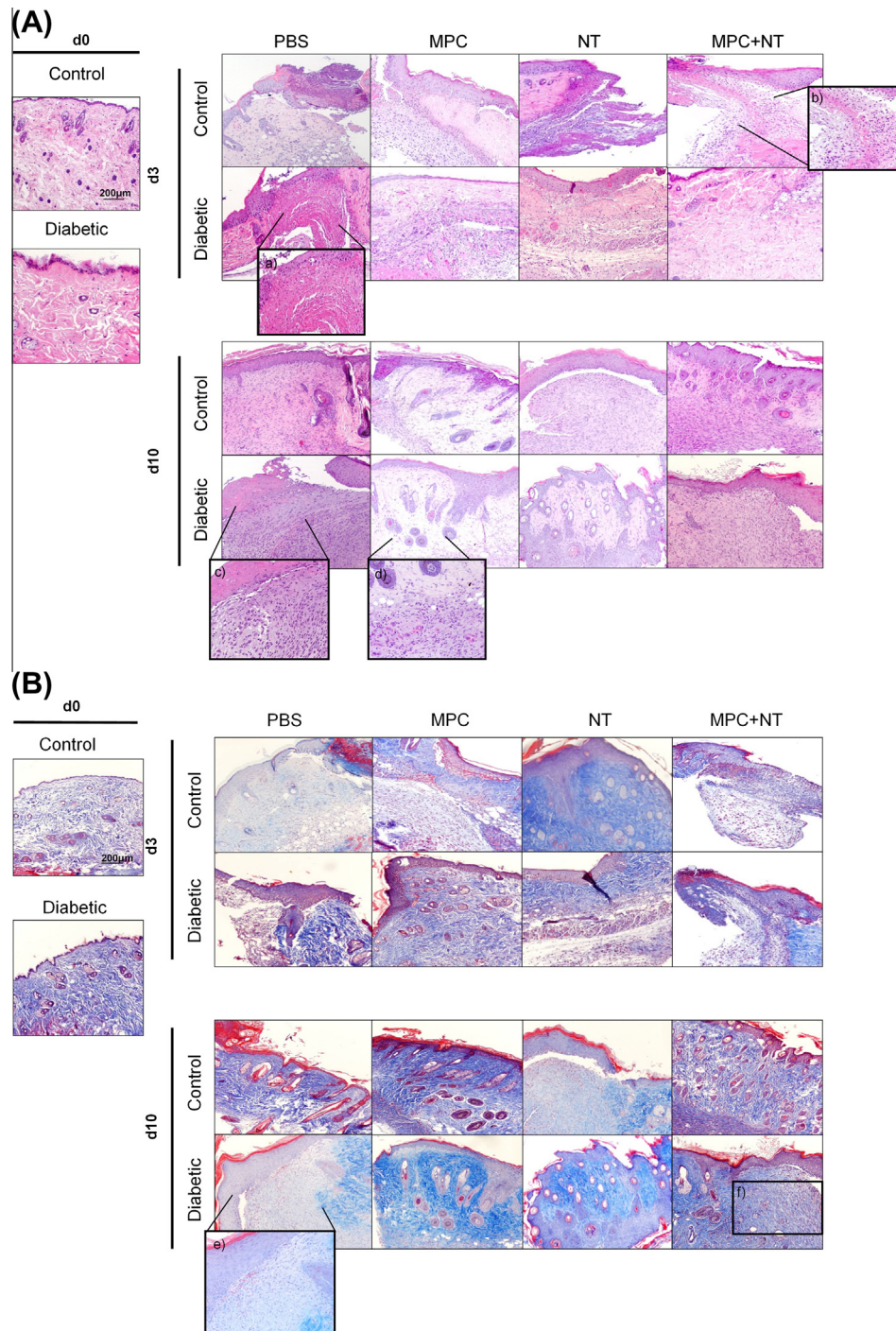
Fig. 9. Histopathological analysis of (A) hematoxylin and eosin (H&E) and (B) Masson's trichrome staining of control and diabetic mouse skin, untreated or treated with MPC, NT and NT-loaded MPC foam (magnification 100×). Representative images of three skin stainings were analyzed. (a) In diabetic wounds granulation tissue is retained in the dermis with overgrowing fibroblast proliferationon day 3 post-wounding (H&E, 200×). (b) Infiltrating PMN and lymphocytes in the granulation tissue in control mice on day 3 post-wounding (H&E, 200×). (c) Persistent inflammatory cells (neutrophils and lympho-plasmocytic cells) in PBS-treated diabetic mice on day 10 post-wounding (H&E, 200×). (d) Fewer inflammatory cells in granulation tissue, compared with (c), in MPC-treated wounds on day 10 post-wounding (H&E, 200×). (e) Less deposition of collagen in PBS-treated diabetic mice on day 10 post-wounding (Masson's trichrome, 200×). (f) The granulation tissue is formed mainly of thin collagen fibers parallel to the epidermis (Masson's trichrome).

were present in higher numbers compared with PBS treatment. It is important to note that inflammatory cells persisted on day 10, especially in the diabetic wounded skin. No fibrin was observed in either control or diabetic skin (Table 4). More fibroblasts, which are important for tissue repair, were present in diabetic skin compared with control wounded skin on day 3. Moreover, collagen matrix production appeared to be more evident in diabetic skin, particularly after NT or NT-loaded MPC foam treatment. However, scarring was more pronounced after these treatments (Table 3). Furthermore, on day 10 the NT-loaded MPC foam induced fibroblast migration and the production of collagen matrix. However, the scar obtained after this treatment was more pronounced

Table 1
Histological analysis of unwounded skin and NT, MPC and NT loaded MPC foams treated wounds at day 3, by H&E staining. − absence or no alterations, + presence < 10%, ++ presence 10%, −50%, n.a, not applicable.

| | Skin control (d0) | | Day 3 | | | | | | | |
| | | | PBS | | MPC | | NT | | MPC + NT | |
	Control	Diabetic	Control	Diabetic	Control	Diabetic	Control	Diabetic	Control	Diabetic
New epidermis thickness										
- Stratus lucidum	−	+	−	+	+	++	−	+	+	++
- Epithelial layers	−	+	−	+	+	++	−	+	+	++
- Basal layer	−	+	−	+	+	++	−	+	+	++
Wound area (mm^2)	26.48 ± 4.22	27.71 ± 5.41	30.30 ± 0.17	29.02 ± 0.32	18.68 ± 0.12	22.64 ± 0.22	24.53 ± 0.31	20.95 ± 0.34	17.80 ± 0.18	16.68 ± 0.17
Re-epithelization										
- From bottom	na	na	+	−	+	−	+	−	+	−
- Top cover	na	na	−	+	−	+	−	+	−	+

Table 2
Histological analysis of NT, MPC and NT loaded MPC foams treated wounds at day 10, by H&E staining. − absence or no alterations, + presence < 10%, ++ presence 10%, −50%, +++ presence >50%.

| | Day 10 | | | | | | | |
| | PBS | | MPC | | NT | | MPC + NT | |
	Control	Diabetic	Control	Diabetic	Control	Diabetic	Control	Diabetic
New epidermis thickness								
- Stratus lucidum	++	+++	+	++	++	+++	+	++
- Epithelial layers	++	+++	+	++	++	+++	+	++
- Basal layer	++	+++	+	++	++	+++	+	++
Wound area (mm^2)	9.02±0.15	13.39±0.31	4.22±0.09	12.11±0.20	7.05±0.30	9.12±0.30	5.88±0.12	9.77±0.29
Re-epithelization								
- From bottom	+	−	+	−	+	−	+	−
- Top cover	−	+	−	+	−	+	−	+

Table 3
Inflammatory and granulation tissue histological analysis of NT, MPC and NT loaded MPC foams treated wounds at day 3, by H&E and Massoń́s Trichrome staining. − absence or no alterations, +presence <10%, ++ presence 10%, −50%, +++ presence > 50%; < not relevant, > predominant.

| | Day 3 | | | | | | | |
| | PBS | | MPC | | NT | | MPC + NT | |
	Control	Diabetic	Control	Diabetic	Control	Diabetic	Control	Diabetic
Inflammation Status								
- PMN	++	+++	++	+	++	+	++	+
- Lymphocytes	+	++	+	−	+	−	+	−
- Plasma cells	−	−	−	−	−	−	−	−
- Fibrin	<	>	>	<	>	<	>	<
Repair								
- Fibroblasts	<	>	<	>	<	>	<	>
Collagen matrix								
- Loose	−	−	−	+	+	+	+	−
- Scar	−	−	−	+	−	+	+	++

(Table 4). A summary of cytokine expression and corresponding cell type production in wounded control and diabetic skin on days 3 and 10 post-wounding is presented in Table 5.

4. Discussion

One of the main objectives of this work was to evaluate the capacity of chitosan-based wound dressings as biocompatible and biodegradable supports for the sustained delivery of NT, a neuropeptide that has been shown to improve wound healing [27,28].

Three different water-soluble chitosan derivatives (CMC, MPC and SC) were synthesized and tested for their water swelling capacities and peptide release profiles in order to infer which of the derivatives would have the best performance (controlled swelling and NT delivery over time) in vivo. GSH was used as a model peptide. Although GSH has a lower molecular weight than NT, it has similar functional groups that permit simulation of the physical and chemical interactions that may be established between the molecule and the material used as the dressing.

The results obtained showed that the SC foam had the highest water vapor and water swelling capacity, probably due to the high number of thin fibers that constitute the matrix, increasing the contact area between the material and water molecules. The higher affinity of SC for water (higher hydrophilicity) accounts for its faster dissolution in PBS. These results are also in agreement with the

Table 4

Inflammatory and granulation tissue histological analysis of NT, MPC and NT loaded MPC foams treated wounds at day 10, by H&E and Massoń Trichrome staining. − absence or no alterations, + presence <10%, ++ presence 10%,-50%, +++ presence >50%.

	Day 10							
	PBS		MPC		NT		MPC + NT	
	Control	Diabetic	Control	Diabetic	Control	Diabetic	Control	Diabetic
Inflammation Status								
- PMN	−	++	−	+	−	+	−	+
- Lymphocytes	+	+++	+	++	+	++	+	++
- Plasma cells	+	+++	+	++	+	++	+	++
- Fibrin	−	−	−	−	−	−	−	−
Repair								
- Fibroblasts	++	+	+	++	+	+	+	+++
Collagen matrix								
- Loose	−	−	−	−	−	−	−	−
- Scar	++	+	+	++	+	+	+	+++

Table 5

Summary of cytokine and protein expression in wounded control and diabetic skin, at day 3 and 10 post-wounding.

Day	Cytokine/growth factor	Control mice	Diabetic mice	Cell type that produce this protein
3	TNF-α	↓ MPC, NT, MPC+NT	↑ NT, MPC+NT	Macrophages, fibroblasts
	IL-6	↓ MPC; ↑ MPC+NT	↓ MPC, NT, MPC+NT	Macrophages, fibroblasts, Keratinocytes, endothelial cells
	KC	↑ MPC+NT	↓ MPC, NT, MPC+NT	Macrophages, fibroblasts
	IL-1β	↓ MPC, NT, MPC+NT	=MPC, NT, MPC + NT	Macrophages, epithelial cells
	COL1A1	=	↑ NT	Fibroblasts
	COL1A2	=	↑ NT	Fibroblasts
	COL3A1	↑ MPC + NT	↑ NT	Fibroblasts
10	TNF-α	↑ NT, MPC + NT	↓ NT, MPC + NT	Macrophages, fibroblasts
	IL-6	=	↓ MPC, NT, MPC + NT	Macrophages, fibroblasts, keratinocytes, endothelial cells
	KC	=	↓ MPC, NT, MPC + NT	Macrophages, fibroblasts
	IL-1β	=	=	Macrophages, epithelial cells
	COL1A1	↑NT,MPC + NT	↑MPC + NT	Fibroblasts
	COL1A2	↑NT,MPC + NT	↑MPC + NT	Fibroblasts
	COL3A1	↑NT	↑MPC + NT	Fibroblasts

^{1}H NMR data that showed a higher degree of substitution of SC. This was expected since the chitosan substitutions performed in this work were designed to improve the solubility of chitosan in aqueous media. MPC presented an intermediate swelling profile, despite the apparent greater porosity of the CMC derivative observed by SEM analysis.

Medicated wound dressings have largely been used to deliver healing enhancers and therapeutic substances, such as growth factors or stem cells, to stimulate wound healing [29,30]. Their use allows protection of the wound against external factors and avoids rapid biodegradation of the bioactive healing enhancers that may occur in the enzyme-rich wound environment. In this work the capacity of each dressing to sustain the release of a peptide under different pH conditions was addressed. The measured release kinetics were not significantly affected within the pH range studied. SC presented faster release of GSH, followed by MPC and CMC. The release profiles are in accord with the water swelling profiles observed for the different chitosan derivatives, indicating that GSH release is mainly controlled by the water swelling capacity of the material and GSH is mainly released through diffusion. The higher swelling capacity of SC leads to a greater amount of water inside the polymer structure and thus better GSH dissolution, enhancing its release into the surrounding medium. According to these results (water swelling and GSH release data), and considering that sustained release is desirable for in vivo applications, the SC-based material was discarded at this stage.

The biocompatibility of the CMC and MPC foams was tested in vitro, in the Raw 264.7 and HaCaT cell lines. The results showed that both materials were non-toxic against these cell lines up to 48 h. After 72 h a slight decrease (not statistically significant) in viability of the cells was observed, probably due to foam

dissolution or cell stress in the medium conditions. Similar results were observed in L929 cells (a fibroblast cell line) by Huang et al. [31]. The production of nitrites by Raw 264.7 macrophages was also quantified, since it is known that these cells produce NO when subjected to inflammatory stimulus. The results showed that CMC and MPC do not increase nitrite levels in vitro, suggesting that these compounds do not induce an inflammatory response, which is in agreement with data previously reported in the literature [32]. The in vitro results indicate that both CMC and MPC could be used for wound dressing applications. However, in this work in vivo application and characterization was performed only for MPC, the material that presented an intermediate GSH release profile compared with CMC and SC.

Several studies have suggested that chitosan and its derivatives accelerate wound healing [33,34]. For instance, freeze-dried MPC foams were shown to jellify in contact with biological fluids, being progressively absorbed via enzymatic hydrolysis, promoting regeneration of connective tissue [35]. However, no studies reporting the effect of MPC alone or in combination with NT on diabetic wound healing have been found in the literature.

Diabetes mellitus has important complications at the skin level. The healing process involves several overlapping phases: homeostasis/coagulation, inflammation, proliferation (granulation tissue formation), re-epithelialization and remodeling [36]. All of these processes require the interaction of skin cells, cytokines and growth factors released from inflammatory cells, fibroblasts, keratinocytes and epithelial cells [2].

Due to the fact that mouse skin is elastic and lacks strong adherence to the underlying structures, wound contraction is usually more rapid than epithelialization, which causes a decrease in the overall healing time of mouse wounds [37]. Wound closure results

show that NT induced more rapid closure in diabetic mice, even when applied directly over the wound, compared with control mice. This was expected, since it has been reported that topical application of neuropeptides, such as substance P, stimulate diabetic wound healing [9]. In addition, previous studies by our group observed that NT modulates inflammatory responses in a skin dendritic cell line [28]. Treatment with non-loaded and NT-loaded MPC foams induced a significant reduction in the wound area, especially in the first 3 days post-wounding, in both control and diabetic mice. Moreover, NT-loaded MPC presented a faster healing profile in diabetic skin wounds. These results suggest a synergistic behavior between the bioactivity of NT alone and the intrinsic healing properties of MPC. Moreover, and as intended, sustained release of NT may also occur, which guarantees controlled NT levels during the healing process. The adhesive properties of chitosan and its derivatives could explain this enhanced healing profile [38]. In addition, wound contraction is necessary for the healing process, probably due to enhanced proliferation of fibroblasts caused by contractile myofibroblasts [39]. Wound contraction is a biologically important process in wound healing, especially in the healing of chronic wounds such as DFU, although excessive contraction may lead to scar formation [40]. All treatments led to healing, however, larger scars developed over diabetic wounds that were treated with the MPC foams, most probably due to the rapid initial wound contraction verified in this case.

Overexpression of inflammatory cytokines, growth factors and MMP-9 was observed in unwounded diabetic skin, which is in agreement with the literature [41]. These results suggest a chronic pro-inflammatory state in diabetic skin that can compromise wound healing. On the other hand, the gene expression of different types of collagen was down-regulated in diabetic skin, suggesting a decreased capacity of diabetic skin to produce the appropriate matrix essential for wound healing and skin repair. As expression of COL1A1, COL1A2 and COL3A1 is decreased less collagen is deposited, as observed by the hydroxyproline assay [42].

In chronic diabetes the healing process becomes stalled in one or more of the healing phases, resulting in chronic non-healing wounds. One important phase that can become stalled in diabetes is the inflammatory phase [1]. TNF-α, IL-6, IL-8 and IL-1β are inflammatory cytokines involved in the recruitment of cells such as neutrophils and macrophages to the wound site, which stimulate an immune response. In the skin TNF-α produced by inflammatory cells and fibroblasts stimulates adhesion molecules and chemokines, leading to the attachment of inflammatory cells to vessels, migration, and eventually chemotaxis into the skin [43]. IL-6 and IL-1β, produced by macrophages, fibroblasts, keratinocytes and epithelial cells, are also important players in the early phase of inflammation and in the wound healing process [44]. In control mice a reduction in TNF-α and IL-1β expression after all treatments on day 3 suggests decreased inflammation, which facilitates healing. In diabetic mice treated with MPC, NT or NT-loaded MPC fewer infiltrating inflammatory cells were observed on day 3 compared with control mice, while TNF-α expression was significantly higher, especially for MPC alone. Moreover, IL-6 and IL-8 expression were significantly reduced. These results suggest that high expression of TNF-α is not only by inflammatory cells present at the wound site but also by other cells present on day 3, which can stimulate contraction of the wound and consequently have a beneficial effect in the early stages of wound healing. This may further indicate that in diabetic mice treated with NT or/and MPC granulation tissue fills the wound bed in the early phase of wound healing, potentiated by the proliferation of skin fibroblasts.

Similar results were observed when using MPC alone as a treatment. However, NT-loaded MPC treatment induced a decrease in TNF-α protein content, suggesting that the combination of NT with

the MPC foam plays an effective anti-inflammatory role in wound healing.

On day 10 the inflammatory status persisted in diabetic mice, while in the controls it was resolved, as expected [4]. On the other hand, all treatments led to a reduction in inflammatory cytokine expression, supported by the loose conjunctive tissue observed from the beginning, with different levels of collagen deposition in diabetic and control mice. At this time point fibroblasts play an important role in collagen synthesis and scar formation [45,46]. During the re-epithelialization phase the initial ECM is gradually replaced by a collagenous matrix with the formation of new blood vessels [47]. Expression of the angiogenic factors VEGF and PDGF did not change with treatment in diabetic mice, possibly showing that these treatments do not stimulate the production of growth factors to improve wound healing.

Our results show that production of the collagen matrix was higher in MPC and NT-loaded MPC treated diabetic skin, which correlates with increased scar formation. Obara et al. [29] also observed that application of a chitosan hydrogel to diabetic wounds increased scar formation. Moreover, MMP-9 expression in diabetic skin wound was increased on day 3. Most importantly, on day 10 a decrease in MMP-9 was observed in NT-loaded MPC treated diabetic wounds, while no significant effect was observed in control wounds. MMP-9 may possibly affect ECM proteolytic enzymes, allowing migration of cells into the wound site, resulting in the deposition of new ECM and the development of new tissue. However, it is known that increased levels of TNF-α in diabetes could alter the balance of MMP-9/TIMP-2 production by fibroblasts, contributing to elevated proteolytic activity and impairing wound healing [48].

As expected, and in agreement with the literature [49], type 1 collagen was the most expressed form of collagen in the skin, serving as the framework for connective tissues such as skin, bone and tendons. This result also agrees with the observed increase in expression of TGF (Supplementary Fig. S3), which plays an important role in the pathophysiology of tissue repair by enhancing type 1 collagen gene expression [50].

In addition, on day 3 we observed increased expression of all types of collagen in the control compared with diabetic skin at the same time point. The opposite was seen on day 10, suggesting that diabetes impairs collagen gene expression and deposition in the skin [51]. Moreover, the NT-loaded MPC foam stimulated COL1A1, COL1A2 and COL3A1 expression on day 10 in diabetic skin, which is also correlated with higher collagen production, as observed by the hydroxyproline content and Masson's trichrome staining.

5. Conclusions

The results obtained in this work show that in control animals both MPC and NT-loaded MPC foams have a significant impact on the early phases of the healing process, decreasing the amount of inflammatory infiltrate. In diabetic animals the major healing effects were observed with either NT alone or NT-loaded MPC foams, thus confirming the potential healing effect of NT on diabetic wounds. These treatments reduced the inflammatory status in the early phase of wound healing and increased the migration of fibroblast and collagen expression and deposition for tissue repair. However, a more pronounced scar was observed after the application of MPC. Table 5 summarizes cytokine expression in wounded control and diabetic skin on days 3 and 10 post-wounding.

These results suggest that in vivo application of NT combined with an MPC foam as diabetic wound dressings can promote an inflammatory response, reduce the inflammatory response, promote an anti-inflammatory response and stimulate re-epitheliali-

zation, which are important phases in the healing process. Human studies are needed to further investigate the potential application of NT-loaded MPC wound dressings as a therapy for DFUs.

6. Conflict of interest

The authors declare no competing financial interests.

Appendix A. Supplementary data

Supplementary data associated with this article can be found, in the online version, at http://dx.doi.org/10.1016/j.actbio.2013.09.040.

Appendix B. Figures with essential color discrimination

Certain figures in this article, particularly Fig. 9, are difficult to interpret in black and white. The full color images can be found in the on-line version, at http://dx.doi.org/10.1016/j.actbio.2013.09.040.

References

[1] Moura LI, Dias AM, Carvalho E, de Sousa HC. Recent advances on the development of wound dressings for diabetic foot ulcer treatment – a review. Acta Biomaterialia 2013;9:7093–114.
[2] Tellechea A, Leal E, Veves A, Carvalho E. Inflammatory and angiogenic abnormalities in diabetic wound healing: role of neuropeptides and therapeutic perspectives. Open Circ Vasc J 2010;3:43–55.
[3] Silva L, Carvalho E, Cruz MT. Role of neuropeptides in skin inflammation and its involvement in diabetic wound healing. Expert Opin Biol Ther 2010;10:1427–39.
[4] Pradhan L, Nabzdyk C, Andersen ND, LoGerfo FW, Veves A. Inflammation and neuropeptides: the connection in diabetic wound healing. Expert Rev Mol Med 2009;11:e2.
[5] Lazarus LH, Brown MR, Perrin MH. Distribution, localization and characteristics of neurotensin binding sites in the rat brain. Neuropharmacology 1977;16:625–9.
[6] Sundler F, Hakanson R, Hammer RA, Alumets J, Carraway R, Leeman SE, et al. Immunohistochemical localization of neurotensin in endocrine cells of the gut. Cell Tissue Res 1977;178:313–21.
[7] Brain SD. Sensory neuropeptides: their role in inflammation and wound healing. Immunopharmacology 1997;37:133–52.
[8] Kalafatakis K, Triantafyllou K. Contribution of neurotensin in the immune and neuroendocrine modulation of normal and abnormal enteric function. Regul Pept 2011;170:7–17.
[9] Scott JR, Tamura RN, Muangman P, Isik FF, Xie C, Gibran NS. Topical substance P increases inflammatory cell density in genetically diabetic murine wounds. Wound Repair Regen 2008;16:529–33.
[10] Pradhan L, Cai X, Wu S, Andersen ND, Martin M, Malek J, et al. Gene expression of pro-inflammatory cytokines and neuropeptides in diabetic wound healing. J Surg Res 2011;167:336–42.
[11] Sweitzer SM, Fann SA, Borg TK, Baynes JW, Yost MJ. What is the future of diabetic wound care? Diabetes Educ 2006;32:197–210.
[12] Malafaya PB, Silva GA, Reis RL. Natural-origin polymers as carriers and scaffolds for biomolecules and cell delivery in tissue engineering applications. Adv Drug Deliv Rev 2007;59:207–33.
[13] Sell SA, Wolfe PS, Garg K, McCool JM, Rodriguez IA, Bowlin GL. The use of natural polymers in tissue engineering: a focus on electrospun extracellular matrix analogues. Polym Adv Technol 2010;2:522–53.
[14] Rinaudo M. Chitin and chitosan: properties and applications. Polym Adv Technol 2006;31:603–32.
[15] Park CJ, Clark SG, Lichtensteiger CA, Jamison RD, Johnson AJW. Accelerated wound closure of pressure ulcers in aged mice by chitosan scaffolds with and without bFGF. Acta Biomater 2009;5:1926–36.
[16] Huang S, Fu X. Naturally derived materials-based cell and drug delivery systems in skin regeneration. J. Controlled Release 2010;142:149–59.
[17] Dai T, Tanaka M, Huang YY, Hamblin MR. Chitosan preparations for wounds and burns: antimicrobial and wound-healing effects. Expert Rev Anti Infect Ther 2011;9:857–79.
[18] Takei T, Nakahara H, Ijima H, Kawakami K. Synthesis of a chitosan derivative soluble at neutral pH and gellable by freeze-thawing, and its application in wound care. Acta Biomater 2012;8:686–93.
[19] Berscht PC, Nies B, Liebendorfer A, Kreuter J. Incorporation of basic fibroblast growth factor into methylpyrrolidinone chitosan fleeces and determination of the in vitro release characteristics. Biomaterials 1994;15:593–600.
[20] Dai YN, Li P, Zhang JP, Wang AQ, Wei Q. A novel pH sensitive N-succinyl chitosan/alginate hydrogel bead for nifedipine delivery. Biopharm Drug Dispos 2008;29:173–84.
[21] Tan Y, Han F, Ma S, Yu W. Carboxymethyl chitosan prevents formation of broad-spectrum biofilm. Carbohydr Polym 2011;84:1365–70.
[22] Chen X, Wang Z, Liu W, Park H. The effect of carboxymethyl-chitosan on proliferation and collagen secretion of normal and keloid skin fibroblasts. Biomaterials 2002;23:4609–14.
[23] Prabaharan M. Review paper: chitosan derivatives as promising materials for controlled drug delivery. J Biomater Appl 2008;23:5–38.
[24] Muzzarelli RAA, Ilari P, Tomasetti M. Preparation and characteristic properties of 5-methyl pyrrolidinone chitosan. Carbohydr Polym 1993;20:99–105.
[25] Santos KSCR, Silva HSRC, Ferreira EI, Bruns RE. 32Factorial design and response surface analysis optimization of N-carboxybutylchitosan synthesis. Carbohydr Polym 2005;59:37–42.
[26] Dias AMA, Rey-Ricob A, Oliveira RA, Marceneiro S, Alvarez-Lorenzo C, Concheiro A, et al. Wound dressings loaded with an anti-inflammatory jucá (Libidibia ferrea) extract using supercritical carbon dioxide technology. J Supercrit Fluids 2013;74:34–45.
[27] Brun P, Mastrotto C, Beggiao E, Stefani A, Barzon L, Sturniolo GC, et al. Neuropeptide neurotensin stimulates intestinal wound healing following chronic intestinal inflammation. Am J Physiol Gastrointest Liver Physiol 2005;288:G621–629.
[28] da Silva L, Neves BM, Moura L, Cruz MT, Carvalho E. Neurotensin downregulates the pro-inflammatory properties of skin dendritic cells and increases epidermal growth factor expression. Biochim Biophys Acta 2011;1813:1863–71.
[29] Obara K, Ishihara M, Fujita M, Kanatani Y, Hattori H, Matsui T, et al. Acceleration of wound healing in healing-impaired db/db mice with a photocrosslinkable chitosan hydrogel containing fibroblast growth factor-2. Wound Repair Regen 2005;13:390–7.
[30] Rossi S, Marciello M, Sandri G, Ferrari F, Bonferoni MC, Papetti A, et al. Wound dressings based on chitosans and hyaluronic acid for the release of chlorhexidine diacetate in skin ulcer therapy. Pharm Dev Technol 2007;12:415–22.
[31] Huang P, Han B, Liu W, Chang Q, Dong W. Preparation and biocompatibility of N-carboxymethyl chitosan. J Funct Mater 2009;7:25–33.
[32] Hwang SM, Chen CY, Chen SS, Chen JC. Chitinous materials inhibit nitric oxide production by activated RAW 264.7 macrophages. Biochem Biophys Res Commun 2000;271:229–33.
[33] Yang C, Zhou Y, Zhang X, Huang X, Wang M, Han Y, et al. A green fabrication approach of gelatin/CM-chitosan hybrid hydrogel for wound healing. Carbohydr Polym 2010;82:1297–305.
[34] Chen R, Wang G, Chen C, Ho H, Shen M. Development of a new N-O-(carboxymethyl)/chitosan/collagen matrixes as a wound dressing. Biomacromolecules 2006;7:1058–64.
[35] Muzzarelli R. Depolymerization of methyl pyrrolidinone chitosan by lysozyme. Carbohydr Polym 1992;19:29–34.
[36] Enoch S, Leaper DJ. Basic science of wound healing. Surgery 2008;26:31–7.
[37] Davidson JM. Animal models for wound repair. Arch Dermatol Res 1998;290(Suppl.):S1–S11.
[38] Lehr C, Bouwstra JA, Schacht EH, Junginger HE. In vitro evaluation of mucoadhesive properties of chitosan and some other natural polymers. Int J Pharm 1992;78:43–8.
[39] Ono I, Tateshita T, Inoue M. Effect of a collagen matrix containing basic fibroblast growth factor on wound contraction. J Biomed Mater Res Appl Biomater 1999;48:621–30.
[40] Ishihara M, Ono K, Sato M, Nakanishi K, Saito Y, Yura H, et al. Acceleration of wound contraction and healing with a photocrosslinkable chitosan hydrogel. Wound Repair Regen 2001;9:513–21.
[41] Galkowska H, Wojewodzka U, Olszewski WL. Chemokines, cytokines, and growth factors in keratinocytes and dermal endothelial cells in the margin of chronic diabetic foot ulcers. Wound Repair Regen 2006;14:558–65.
[42] Hansen SL, Myers CA, Charboneau A, Young DM, Boudreau N. HoxD3 accelerates wound healing in diabetic mice. Am J Pathol 2003;163:2421–31.
[43] Bashir MM, Sharma MR, Werth VP. TNF-alpha production in the skin. Arch Dermatol Res 2009;301:87–91.
[44] Lin Z, Kondo T, Ishida Y, Takayasu T, Mukaida N. Essential involvement of IL-6 in the skin wound-healing process as evidenced by delayed wound healing in IL-6 deficient mice. J Leukoc Biol 2003;73:713–21.
[45] Gabbiani G. The myofibroblast in wound healing and fibrocontractive diseases. J Pathol 2003;200:500–3.

[46] Diegelmann RF, Evans MC. Wound healing: an overview of acute, fibrotic and delayed healing. Front Biosci 2004;9:283–9.

[47] Singer AJ, Clark RA. Cutaneous wound healing. N Engl J Med 1999;341:738–46.

[48] Blakytny R, Jude EB. Altered molecular mechanisms of diabetic foot ulcers. Int J Low Extrem Wounds 2009;8:95–104.

[49] Crane NJ, Brown TS, Evans KN, Hawksworth JS, Hussey S, Tadaki DK, et al. Monitoring the healing of combat wounds using Raman spectroscopic mapping. Wound Repair Regen 2010;18:409–16.

[50] Verrecchia F, Mauviel A. TGF-beta and TNF-alpha: antagonistic cytokines controlling type I collagen gene expression. Cell Signal 2004;16:873–80.

[51] Black E, Vibe-Petersen J, Jorgensen LN, Madsen SM, Agren MS, Holstein PE, et al. Decrease of collagen deposition in wound repair in type 1 diabetes independent of glycemic control. Arch Surg 2003;138:34–40.